Tuning the Excited-State Properties of Luminescent Rhenium(V) Benzylidyne Complexes Containing Phosphorus and Nitrogen Donor Ligands

Wen-Mei Xue, Yue Wang, Michael Chi-Wang Chan, Zhong-Min Su, Kung-Kai Cheung, and Chi-Ming Che*

Department of Chemistry, The University of Hong Kong, Pokfulam Road, Hong Kong

Received December 2, 1997

Efficient methods are developed for the synthesis of rhenium(V)-substituted benzylidyne complexes with various auxiliary ligands to facilitate the tuning of their excited-state properties. The electronic structures and spectroscopic and photophysical properties of [Re(≡CAr′)(pdpp)$_2$Cl]$^+$ (Ar′ = $C_6H_2Me_3$-2,4,6, pdpp = *o*-phenylenebis(diphenylphosphine), **2**), [Re(≡CAr′)L$_2$(CO)(H$_2$O)Cl]$^+$ (L = PPh_3, **3**; P(C_6H_4OMe-*p*)$_3$, **4**; PPh_2Me, **5**), [Re(≡CAr′)(dppe)(CO)$_2$Cl]$^+$ (dppe = 1,2-bis(diphenylphosphino)ethane, **6**), [Re(≡CAr′)(L−L)(CO)$_2$Cl]$^+$ (L−L = 2,2′-bipyridine, **7**; 4,4′-dichloro-2,2′-bipyridine, **8**; 4,4′-dimethoxycarbonyl-2,2′-bipyridine, **9**), [Re(≡CAr′)(Tp′)(CO)$_2$]$^+$ (Tp′ = tris(3,5-dimethyl-1-pyrazolyl)borohydride, **10**), and [Re(≡CC_6H_4-R)(pdpp)(CO)$_2$(O_3SCF_3)]$^+$ (**13**, R = OMe, **a**; Me, **b**; H, **c**; Cl, **d**; Br, **e**; CN, **f**) are studied and compared. The molecular structures of **7**·$CHCl_3$, **10**, **12f**, **13a**·CH_3OH·H_2O, and **13d**·2CH_2Cl_2 are determined by X-ray crystallography and reveal Re≡C distances in the 1.766(8)−1.786(7) Å range. HF-SCF calculations on the model compounds [Re(≡CC_6H_5)(H_2PCH=CHPH_2)$_2$Cl]$^+$ (**2m**), [Re(≡CC_6H_5)(PH_3)$_2$(H$_2$O)(CO)Cl]$^+$ (**3m**), and [Re(≡CC_6H_5)(H_2PCH=CHPH_2)(CO)$_2$(OH)]$^+$ (**13m**) suggest that the HOMO is π(Re≡C−Ph) and the LUMO is π*(Re≡C−Ph). CI-singles calculations on the excited state of optimized **2m** indicate that the lowest energy UV−vis absorption of **2**−**6**, **10**, and **13** originates from a HOMO to LUMO spin-forbidden transition. This is identified as ^{3}[π(Re≡CAr) → π*(Re≡CAr)], where d(Re) → p(≡C) MLCT character is apparent and the p(≡C) orbital and phenyl π system are conjugated. The UV−vis absorption spectra of **7**−**9** are significantly different, and their lowest energy absorption is assigned d(Re) → π*(X_2-bpy). The rhenium(V) benzylidyne complexes are highly emissive at room temperature and 77 K. The combination of spectroscopic studies and theoretical calculations suggest that the emitting state of **2**−**6**, **10**, and **13** is ^{3}[π(Re≡CAr)→π*(Re≡CAr)] but that of **7**−**9** is d(Re) → π*(X_2-bpy). The emission energies in dichloromethane can be adjusted from 520 to 610 nm by variation of the benzylidyne and ancillary ligands. Their electrochemical behaviors are examined and provide further evidence to support the excited-state assignment.

Introduction

Fluid luminescence from metal alkylidyne complexes was first observed in 1985.[1] However, emissive complexes containing a metal−carbon triple bond remain rare. To our knowledge, the only reported examples are the d^2 species [W(≡CPh)(L$_2$)X(CO)$_2$] (L$_2$ = tmen (*N*,*N*,*N*′,*N*′-tetramethylethylenediimine), (py)$_2$, dppe (1,2-bis(diphenylphosphino)ethane); X = Cl, Br, I),[1] Cp(CO)[P(OMe)$_3$]M≡CR (M = Mo, W; R = Ph, *o*-tolyl),[2] and [Os(≡CPh)(NH_3)$_5$](O_3SCF_3)$_3$[3] and the d^1 derivatives Re(≡CAr′)(PPh_3)(H$_2$O)X$_3$ (Ar′ = 2,4,6-$C_6H_2Me_3$; X = Cl, Br).[4] Hopkins has studied the molecular structures of the redox compounds W(≡CPh)(dmpe)$_2$Br and [W(≡CPh)(dmpe)$_2$Br][PF_6], and examination of their electronic absorption spectra at high resolution provided a direct assignment of the frontier molecular orbitals.[5] McElwee-White reported the observation of the lowest excited states of tungsten and molybdenum arylcarbyne complexes by laser flash photolysis.[6] A number of accounts on alkylidyne/carbyne-based photochemical reactions have appeared,[7] although the nature of the excited states remains elusive.

Following the work by Schrock and Williams on d^2 rhenium benzylidyne complexes,[8] our studies have revealed that congeners bearing phosphine ligands exhibit a long-lived emissive excited state in fluid solution.[9] We have continued to develop this theme with the purpose of (1) defining the nature of the emissive excited state in order to gain further insight into the photochemistry of metal benzylidyne complexes

(1) Bocarsly, A. B.; Cameron, R. E.; Rubin, H. D.; McDermott, G. A.; Wolff, C. R.; Mayr, A. *Inorg. Chem.* **1985**, *24*, 3976.
(2) Carter, J. D.; Kingsburg, K. B.; Wilde, A.; Schoch, T. K.; Leep, C. J.; Pham, E. K.; McElwee-White, L. *J. Am. Chem. Soc.* **1991**, *113*, 2947.
(3) Trammell, S.; Sullivan, B. P.; Hodges, L. M.; Harman, W. D.; Smith, S. R.; Thorp, H. H. *Inorg. Chem.* **1995**, *34*, 2791.
(4) Xue, W. M.; Chan, M. C. W.; Mak, T. C. W.; Che, C. M. *Inorg. Chem.* **1997**, *36*, 6437.
(5) Manna, J.; Gilbert, T. M.; Dallinger, R. F.; Geib, S. J.; Hopkins, M. D. *J. Am. Chem. Soc.* **1992**, *114*, 5870.
(6) Schoch, T. K.; Main, A. D.; Burton, R. D.; Lucia, L. A.; Robinson, E. A.; Schanze, K. S.; McElwee-White, L. *Inorg. Chem.* **1996**, *35*, 7769.

S0276-7333(97)01054-6 CCC: $15.00
Publication on Web 04/14/1998

and (2) exploring the relationship between molecular structure and excited-state properties, such as excited-state energy, nonradiative and radiative decay rate constants, and excited-state redox potentials. A key component of this work is the convenient synthesis of a series of rhenium(V)-substituted benzylidyne complexes with different ancillary ligands. Rhenium alkylidyne complexes are relatively rare compared to the group 6 analogues,[10] and previous routes do not allow for the modification of both the alkylidyne and auxiliary groups. We now present synthetic strategies to two series of luminescent rhenium(V) benzylidyne complexes: (1) 2,4,6-trimethylbenzylidyne species containing various phosphorus or nitrogen donor ligands (**2**−**10**) and (2) para-substituted benzylidyne derivatives supported by *o*-phenylenebis(diphenylphosphine) (pdpp) (**13a**−**f**). Detailed spectroscopic investigations demonstrate that the anticipated tuning of the excited-state properties in these complexes is possible.

Experimental Section

Spectroscopic Procedures. Infrared spectra were recorded with KBr disks on a BIO-RAD FTS165 FT-IR spectrophotometer. Mass spectra were obtained on a Finnigan Mat 95 mass spectrometer. Elemental analyses were performed by Butterworth Laboratory, U.K. ^{1}H, ^{13}C, and ^{31}P NMR spectra (ppm, in $CDCl_3$ unless otherwise stated) were obtained on a JEOL 270 or a Bruker DRX 300 or 500 multinuclear FT-NMR spectrometer with tetramethylsilane (^{1}H and ^{13}C NMR) and H_3PO_4 (^{31}P NMR) as internal references. UV−vis absorption spectra were obtained on a Milton Roy Spectronic 3000 diode-array spectrophotometer.

Emission Spectra and Lifetimes. Steady-state emission spectra were recorded on a SPEX 1681 FLOUROLOG-2 series F111AI spectrometer and corrected for monochromator and photomultiplier efficiency and xenon lamp stability. The absolute emission quantum yield was measured by the method of Demas and Crosby[11] using quinine sulfate in 0.1 N sulfuric acid as the standard, where the emission quantum yield is 0.546 with 355 nm excitation.

Emission lifetimes were measured with a Quanta Ray DCR-3 pulsed Nd:YAG laser system (pulse output 355 nm, 8 ns). The emission signals were detected by a Hamamatsu R928 photomultiplier tube and recorded on a Tektronix model 2430 digital oscilloscope.

Cyclic Voltammetry. Cyclic voltammetry was performed with a Princeton Applied Research model 175 universal programmer and a model 273 potentiostat. Glassy carbon was used as the working electrode, with Ag−$AgNO_3$ (0.1 mol dm^{-3} in acetonitrile) as the reference electrode and platinum wire as the counter electrode. The supporting electrolyte was *n*-tetrabutylammonium hexafluorophosphate (0.1 mol dm^{-3}). Ferrocene was added as an internal standard.

Materials. 4,4′-Dimethoxycarbonyl-2,2′-bipyridine ((MeO_2C)$_2$-bpy),[12] 4,4′-dichloro-2,2′-bipyridine (Cl_2-bpy),[12] and Re[C(O)Ar′](CO)$_5$[8] were prepared by literature methods. All other reagents were used as received. The synthesis of [Re(≡CAr′)(CO)$_4$Cl][O_3SCF_3] (**1**), [Re(≡CAr′)(pdpp)$_2$Cl][ClO_4] (**2**), [Re(≡CAr′)L_2(CO)(H_2O)Cl]$^+$ (L = PPh_3, **3**; P(C_6H_4OMe-*p*)$_3$, **4**; $PMePh_2$, **5**), and [Re(≡CAr′)(dppe)(CO)$_2$Cl][ClO_4] (**6**) have been reported previously.[9] All manipulations were carried out under a nitrogen atmosphere using standard Schlenk techniques unless otherwise stated.

Syntheses. Satisfactory elemental analysis and infrared and mass spectral data were obtained for all complexes (see Supporting Information).

[Re(≡CAr′)(bpy)(CO)$_2$Cl]ClO_4 (7). A mixture of **1** (0.40 g, 0.65 mmol) and bpy (0.12 g, 0.78 mmol) in toluene (20 cm^3) was refluxed overnight. The resultant pale yellow precipitate was filtered and dissolved in methanol (5 cm^3). $LiClO_4$ (0.5 g) was added to the solution, and precipitation with diethyl ether gave a yellow solid. Recrystallization from an acetonitrile/chloroform mixture afforded golden yellow crystals. Yield: 0.11 g, 25%. ^{1}H NMR (CD_3CN) 2.31 (s, 3, *p*-Me), 2.35 (s, 6, *o*-Me), 6.92 (m, 2, aryl H), 7.85, 8.44, 8.63, 9.34 (4 × m, 8, py H); ^{13}C NMR (CD_3CN) 28.1 (*p*-Me), 30.2 (*o*-Me), 126.0−165.2 (py and aryl C), 207.4, 194.0 (CO).

[Re(≡CAr′)(X_2-bpy)(CO)$_2$Cl]ClO_4 (X = Cl, 8; MeO_2C, 9). A mixture of **1** (0.40 g, 0.65 mmol) and Cl_2-bpy (0.18 g, 0.80 mmol) or (MeO_2C)$_2$-bpy (0.21 g, 0.77 mmol) in tetrahydrofuran (40 cm^3) was refluxed for 16 h. The solvent was removed in vacuo, and the residue was dissolved in methanol (10 cm^3). The crude product was precipitated with $LiClO_4$ (0.5 g) and then diethyl ether. Recrystallization by diffusion of diethyl ether into a chloroform solution gave yellow crystals. Yield: **8**, 0.16 g, 34%; **9**, 0.12 g, 24%.

For **8**: ^{1}H NMR (CD_3CN) 2.16 (s, 3, *p*-Me), 2.25 (s, 6, *o*-Me), 6.89 (s, 2, aryl H), 7.93−8.82 (m, 6, py H); ^{13}C NMR (CD_3CN) 27.4 (*p*-Me), 30.9 (*o*-Me), 125.2−157.7 (m, py and aryl C), 194.4, 207.6 (CO).

For **9**: ^{1}H NMR 2.37 (s, 3, *p*-Me), 2.44 (s, 6, *o*-Me), 4.11 (s, 6, CO_2Me), 6.83 (s, 2, aryl H), 8.16−9.38 (m, 6, py H); ^{13}C NMR 25.1 (*p*-Me), 30.8 (*o*-Me), 54.4 (CO_2*Me*), 124.2−157.6 (m, py and aryl C), 164.5 (CO_2), 194.8, 207.9 (CO).

[Re(≡CAr′)(Tp′)(CO)$_2$][O_3SCF_3] (10). A solution of **1** (0.20 g, 0.36 mmol) and KTp′ (0.14 g, 0.42 mmol) in THF (20 cm^3) was refluxed for 16 h to give a yellow precipitate. This was filtered, washed with THF, and recrystallized by diffusion of diethyl ether into an acetonitrile solution to yield yellow crystals. Yield: 0.064 g, 22%. ^{1}H NMR 2.04 (s, 3, *p*-Me), 2.40−2.47 (m, 24, Tp′ Me and *o*-Me), 6.03 (s, 3, Tp′ H), 6.97 (s, 1, aryl H), 7.05 (s, 1, aryl H); ^{13}C NMR 11.5, 12.6, 12.8, 15.4, 15.9, 18.9 (Tp′-Me), 20.6 (*p*-Me), 22.6 (*o*-Me), 107.8−153.5 (m, Tp′ and aryl C), 192.8 (CO).

Re[C(O)C_6H_4R-*p*](CO)$_5$ (11, R = OCH_3 (a), CH_3 (b), H (c), Cl (d), Br (e), CN (f)). A modified version of Schrock's method was used.[8] $Re_2(CO)_{10}$ (1.0 g, 1.53 mmol) was added to freshly

(7) (a) Mayr, A.; Kjelsberg, M. A.; Lee, K. S.; Asaro, M. F.; Hsieh, T. C. *Organometallics* **1987**, *6*, 2610. (b) Sheridan, J. B.; Pourreau, D. B.; Geoffroy, G. L.; Rheingold, A. L. *Organometallics* **1988**, *7*, 289. (c) Brower, D. C.; Stoll, M.; Templeton, J. L. *Organometallics* **1989**, *8*, 2786. (d) Mayr, A.; Bastos, C. M.; Chang, R. T.; Haberman, J. X.; Robinson, K. S.; Belle-Oudry, D. A. *Angew. Chem., Int. Ed. Engl.* **1992**, *31*, 747. (e) Vogler, A.; Kisslinger, J. Z. *Naturforsch. B.* **1983,** *38B*, 1506. (f) Carter, J. D.; Schoch, T. K.; McElwee-White, L. *Organometallics* **1992**, *11*, 3571. (g) Kingsbury, K. B.; Carter, J. D.; Wilde, A.; Park, H.; Takusagawa, F.; McElwee-White, L. *J. Am. Chem. Soc.* **1993**, *115*, 10056. (h) McElwee-White, L.; Kingsbury, K. B.; Carter, J. D. *Adv. Chem. Ser.* **1993**, *238*, 335.

(8) Williams, D. S.; Schrock, R. R. *Organometallics* **1994**, *13*, 2101.

(9) Xue, W. M.; Wang, Y.; Mak, T. C. W.; Che, C. M. *J. Chem. Soc., Dalton Trans.* **1996**, 2827.

(10) (a) Murdzek, J. S.; Schrock, R. R. In *Carbyne Complexes*; Fischer, H., Hoffman, P., Freissl, F. R., Schrock, R. R., Schubert, U., Weiss, K., Eds.; VCH Verlagsgesellschaft: Weinheim, 1988; p 147ff. (b) LaPointe, A. M.; Schrock, R. R. *Organometallics* **1995**, *14*, 1895. (c) Toreki, R.; Vaughan, A.; Schrock, R. R.; Davis, W. M. *J. Am. Chem. Soc.* **1993**, *115*, 127. (d) Almeida, S. S. P. R.; Frausto Da Silva, J. J. R.; Pombeiro, A. J. L. *J. Organomet. Chem.* **1993**, *450*, C7. (e) Lemos, M. A. N. D. A.; Pombeiro, A. J. L.; Hughes, D. L. R.; Richards, L. *J. Organomet. Chem.* **1992**, *434*, C6. (f) Toreki, R.; Schrock, R. R.; Davis, W. M. *J. Am. Chem. Soc.* **1992**, *114*, 3367. (g) Weinstock, I. A.; Schrock, R. R.; Davis, W. M. *J. Am. Chem. Soc.* **1991**, *113*, 135. (h) Herrmann, W. A.; Felixberger, J. K.; Anwander, R.; Herdtweck, E.; Kiprof, P.; Riede, J. *Organometallics* **1990**, *9*, 1434. (i) Felixberger, J. K.; Kiprof, P.; Herdtweck, E.; Herrmann, W. A.; Jakobi, R.; Gütlich, P. *Angew. Chem., Int. Ed. Engl.* **1989**, *28*, 334. (j) Pombeiro, A. J. L.; Hills, A.; Hughes, D. L.; Richards, R. L. *J. Organomet. Chem.* **1988**, *352*, C5. (k) Pombeiro, A. J. L.; Carvalho, M. F. N. N.; Hitchcock P. B.; Richards, R. L. *J. Chem. Soc., Dalton Trans.* **1981**, 1629.

(11) Demas, J, N.; Crosby, G. A. *J. Phys. Chem.* **1971**, *75*, 991.

(12) Cook, M. J.; Lewis, A. P.; McAnliffe, G. S. G.; Skarda, V.; Thomson, A. J.; Glasper J. L.; Robbins, D. J. *J. Chem. Soc., Perkin Trans. 2* **1984**, 1293.

prepared sodium amalgam (0.1 g of Na, 4.4 mmol, 10 g of Hg) in tetrahydrofuran (40 cm^3), and the mixture was stirred for 12 h at room temperature. The resultant bright orange solution was filtered, and *p*-R-C_6H_4COCl (3.06 mmol, R = OCH_3, 0.52 g; CH_3, 0.40 cm^3; H, 0.36 cm^3; Cl, 0.40 cm^3; Br, 0.67 g; CN, 0.50 g) was added to the filtrate. After 1 h of stirring at room temperature, the mixture was filtered and the solvent was removed in vacuo. Recrystallization of the residue in dichloromethane/methanol afforded yellow crystals.

For **11a**: yield 0.68 g, 48%; ^1H NMR 3.86 (s, 3, CH_3), 6.94 (d, 2, J_{HH} = 9.0, *m*-H), 7.56 (d, 2, J_{HH} = 9.0, *o*-H); ^{13}C NMR 55.5 (OMe), 113.3, 129.6, 146.9, 162.1 (aryl C), 181.2 (ax-CO), 183.1 (eq-CO), 242.2 (C═O).

For **11b**: yield 0.66 g, 48%; ^1H NMR 2.38 (s, 3, CH_3), 7.23 (d, 2, J_{HH} = 8.0, *m*-H), 7.43 (d, 2, J_{HH} = 8.0, *o*-H); ^{13}C NMR 21.3 (CH_3), 127.0, 129.0, 141.5, 151.5 (aryl C), 181.2 (ax-CO), 183.0 (eq-CO), 244.6 (C═O).

For **11c**: yield 0.58 g, 44%; ^1H NMR 7.41−7.50 (m, aryl H); ^{13}C NMR 126.3, 128.4, 130.9, 154.3 (aryl C), 181.1 (ax-CO_{ax}), 182.9 (eq-CO), 246.0 (C═O).

For **11d**: yield 0.69 g, 47%; ^1H NMR 7.42 (m, aryl H); ^{13}C NMR 127.8, 128.6, 137.2, 152.1 (aryl C), 180.8 (ax-CO), 182.7 (eq-CO), 244.1 (C═O).

For **11e**: yield 0.77 g, 49%; ^1H NMR 7.35 (d, 2, J_{HH} = 8.5, *m*-H), 7.58 (d, 2, J_{HH} = 8.3, *o*-H); ^{13}C NMR 126.1, 128.3, 131.9, 132.8 (aryl C), 181.1 (ax-CO), 183.0 (eq-CO), 244.9 (C═O).

For **11f**: yield 0.61 g, 44%; ^1H NMR 7.46 (d, 2, J_{HH} = 8.5, *m*-H), 7.75 (d, 2, J_{HH} = 8.5, *o*-H); ^{13}C NMR 113.8 (CN), 118.3, 125.6, 132.6, 157.0 (aryl C), 180.5 (ax-CO), 182.2 (eq-CO), 245.9 (C═O).

Re[C(O)C_6H_4R-*p*](pdpp)$(CO)_3$ (12, R = OCH_3 (a), CH_3 (b), H (c), Cl (d), Br e), CN (f)). A mixture of Re[C(O)C_6H_4R-*p*]$(CO)_5$ (**11a**−**f**, 0.87 mmol) and pdpp (0.39 g, 0.87 mmol) in tetrahydrofuran (40 cm^3) was refluxed for 12 h. The solvent was removed in vacuo, and the residue was recrystallized in dichloromethane to give yellow to orange crystalline solids.

For **12a**: yield 0.51 g, 69%; ^1H NMR 3.79 (s, 3, CH_3), 6.72−7.78 (m, 28, aryl H); ^{13}C NMR 55.2 (CH_3), 112.2 (*p*-C), 128.0−148.9 (m, aryl C), 160.6 (*ipso*-C), 193.1 (d, $^2J_{CP}$ = 4.6, ax-CO), 196.6 (d, $^2J_{CP}$ = 10.7, eq-CO), 197.3 (d, $^2J_{CP}$ = 10.7, eq-CO), 263.7 (C═O); ^{31}P NMR 44.2.

For **12b**: yield 0.54 g, 74%; ^1H NMR 2.28 (s, 3, CH_3), 7.00−7.79 (m, 28, aryl H); ^{13}C NMR 21.2 (CH_3), 127.2−141.9 (m, aryl C), 153.1 (*ipso*-C), 193.2 (t, $^2J_{CP}$ = 5.4, ax-CO), 196.5 (d, $^2J_{CP}$ = 10.7, eq-CO), 197.2 (d, $^2J_{CP}$ = 10.7, eq-CO), 265.8 (t, $^2J_{CP}$ = 10.7, C═O); ^{31}P NMR 44.2.

For **12c**: yield 0.50 g, 70%; ^1H NMR 7.08−7.80 (m, aryl H); ^{13}C NMR 126.6−141.8 (m, aryl C), 155.5 (*ipso*-C), 193.2 (t, $^2J_{CP}$ = 5.3, ax-CO), 196.2 (d, $^2J_{CP}$ = 10.7, eq-CO), 196.9 (d, $^2J_{CP}$ = 10.7, eq-CO), 268.1 (C═O); ^{31}P NMR 44.1.

For **12d**: yield 0.57 g, 77%; ^1H NMR 7.07−7.79 (m, aryl H); ^{13}C NMR 127.4−141.8 (m, aryl C), 153.6 (*ipso*-C), 193.0 (ax-CO), 196.1 (d, $^2J_{CP}$ = 10.7, eq-CO), 196.9 (d, $^2J_{CP}$ = 10.7, eq-CO), 265.1 (C═O); ^{31}P NMR 44.1.

For **12e**: yield 0.58 g, 74%; ^1H NMR 7.04−7.80 (m, aryl H); ^{13}C NMR 123.7−141.6 (m, aryl C), 154.2 (*ipso*-C), 193.0 (ax-CO), 196.3 (d, $^2J_{CP}$ = 10.2, eq-CO), 196.7 (d, $^2J_{CP}$ = 10.2, eq-CO), 265.1 (C═O); ^{31}P NMR 44.1.

For **12f**: yield 0.53 g, 72%; ^1H NMR 6.95−7.82 (m, aryl-H); ^{13}C NMR 111.6 (CN), 119.1, 125.6−141.6, 158.7 (aryl C), 192.9 (d, $^2J_{CP}$ = 9.1, ax-CO), 195.7 (d, $^2J_{CP}$ = 10.7, eq-CO), 196.5 (eq-CO), 266.3 (C═O); ^{31}P NMR 43.8.

[Re(≡CC_6H_4R-*p*)](pdpp)$(CO)_2(O_3SCF_3)$][O_3SCF_3] (13, R = OCH_3 (a), CH_3 (b), H (c), Cl (d), Br (e), CN (f)). Trifluoromethanesulfonic anhydride (40 mm^3, 0.23 mmol) was added to complexes **12a**−**f** (0.23 mmol) in dichloromethane (10 cm^3) at −40 °C. After 30 min, the volume of the solution was reduced in vacuo at 0 °C to 5 cm^3 and diethyl ether (40 cm^3) was added to precipitate the product. Recrystallization in dichloromethane/diethyl ether/methanol mixtures at −20 °C afforded yellow crystals.

For **13a**: yield 0.08 g, 32%; ^1H NMR 3.89 (s, 3, CH_3), 6.61 (d, 2, J_{HH} = 9.0, *m*-H), 6.71 (d, 2, J_{HH} = 9.0, *o*-H), 7.27−7.98 (m, 24, aryl H); ^{13}C NMR 56.8 (CH_3), 114.9 (CF_3), 126.1−137.9 (m, aryl C), 166.6 (*ipso*-C), 185.6 (d, $^2J_{CP}$ = 8.7, CO), 186.1 (d, $^2J_{CP}$ = 8.4, CO), 301.5 (t, $^2J_{CP}$ = 10.0, Re≡C); ^{31}P NMR 39.7.

For **13b**: yield 0.09 g, 35%; ^1H NMR 2.35 (s, 3, CH_3), 6.12 (d, 2, J_{HH} = 8.2, *m*-H), 6.94 (d, 2, J_{HH} = 8.2, *o*-H), 7.32−8.00 (m, 24, aryl H); ^{13}C NMR 22.8 (CH_3), 126.0−149.8 (m, aryl C), 185.2 (d, $^2J_{CP}$ = 8.3, CO), 185.6 (d, $^2J_{CP}$ = 8.4, CO), 300.4 (t, $^2J_{CP}$ = 10.0, Re≡C); ^{31}P NMR 39.5.

For **13c**: yield 0.08 g, 32%; ^1H NMR 6.20 (d, 2, J_{HH} = 7.3, *m*-H), 6.94 (d, 2, J_{HH} = 7.3, *o*-H), 6.93−8.07 (m, 24, aryl H); ^{13}C NMR 125.8−142.1 (m, aryl C), 184.9 (d, $^2J_{CP}$ = 8.6, CO), 185.4 (d, $^2J_{CP}$ = 8.6, CO), 299.7 (t, $^2J_{CP}$ = 10.1, Re≡C); ^{31}P NMR 39.4.

For **13d**: yield 0.09 g, 36%; ^1H NMR 6.12 (d, 2, J_{HH} = 8.5, *m*-H), 7.05 (d, 2, J_{HH} = 8.5, *o*-H), 7.31−8.00 (m, 24H, aryl H); ^{13}C NMR 125.9−143.7 (m, aryl C), 184.6 (d, $^2J_{CP}$ = 8.2, CO), 185.1 (d, $^2J_{CP}$ = 8.2, CO), 297.6 (t, $^2J_{CP}$ = 10.3, Re≡C); ^{31}P NMR 39.4.

For **13e**: yield 0.09 g, 34%; ^1H NMR 6.06 (d, 2H, J_{HH} = 8.5, *m*-H), 7.24 (d, 2H, J_{HH} = 8.5, *o*-H), 7.38−8.01 (m, 24H, aryl H); ^{13}C NMR 126.0−140.7 (m, aryl C), 184.6 (d, $^2J_{CP}$ = 8.5, CO), 185.1 (d, $^2J_{CP}$ = 8.5, CO), 297.7 (t, $^2J_{CP}$ = 10.2, Re≡C); ^{31}P NMR 39.4.

For **13f**: yield 0.08 g, 30%; ^1H NMR (CD_3CN) 6.74−8.06 (m, aryl H); ^{13}C NMR (CD_3CN) 126.9−145.9 (m, aryl C), 183.4 (d, $^2J_{CP}$ = 8.0, CO), 183.8 (d, $^2J_{CP}$ = 7.8, CO), 302.5 (t, $^2J_{CP}$ = 9.8, Re≡C); ^{31}P NMR (CD_3CN) 39.6.

Structural Determination. Intensity data for **10**, **12f**, **13a**·$CH_3OH·H_2O$, and **13d**·$2CH_2Cl_2$ were collected at 301 K on a Rigaku AFC7R diffractometer with graphite-monochromated Mo Kα radiation (λ = 0.710 73 Å) using ω-2θ scans at a speed of 16.0 deg min^{-1}. Intensity data were corrected for Lorentz and polarization effects. The structures were solved by Patterson methods, expanded by Fourier techniques (*PATTY*[13]), and refined by full-matrix least-squares using the software package *TeXsan*[14] on a Silicon Graphics Indy computer.

Crystallographic data are summarized in Table 1. For complex **10**, a crystallographic asymmetric unit consists of one complex cation and one $CF_3SO_3^-$ anion. All 45 non-H atoms were refined anisotropically, H(1) bonded to B(1) was located in the difference Fourier synthesis and its positional parameters were refined, and 32 H atoms at calculated positions with thermal parameters equal to 1.3 times that of the attached C atoms were not refined. For complex **12f**, all 49 non-H atoms were refined anisotropically, and 28 H atoms at calculated positions were not refined. For complex **13a**·$CH_3OH·H_2O$, all 65 non-H atoms were refined anisotropically and 31 H atoms at calculated positions were not refined. The H atoms of the methanol molecule and water molecule were not located. For complex **13d**·$2CH_2Cl_2$, all 53 non-H atoms of the complex cation, the S atom of the $CF_3SO_3^-$ anion, and the 4 Cl atoms of the dichloromethane molecules were refined anisotropically. The O, F, and C atoms of the anion and solvent molecules were refined isotropically. A total of 33 H atoms at calculated positions with thermal parameters equal to 1.3 times that of the attached C atoms were not refined.

The crystal structures of **7**·$CHCl_3$, **12a**, and **12d** have also been determined and are presented in the Supporting Information. The quality of the crystal data for **7**·$CHCl_3$ was relatively poor and resulted in large standard deviations; nevertheless, its structural parameters are discussed.

(13) Beurskens, P. T.; Admiraal, G.; Beurskens, G.; Bosman, W. P.; Garcia-Granda, S.; Gould, R. O.; Smits, J. M. M.; Smykalla, C. *The DIRDIF program system*; Technical Report of the Crystallography Laboratory; University of Nijmegen: The Netherlands, 1992.

(14) *Crystal Structure Analysis Package*; Molecular Structure Corp.: The Woodlands, TX, 1985 and 1992.

Table 1. Crystallographic Data

	10	**12f**	**13a**·CH_3OH·H_2O	**13d**·$2CH_2Cl_2$
formula	$C_{28}H_{33}N_6O_5BF_3ReS$	$C_{41}H_{28}NO_4P_2Re$	$C_{43}H_{37}O_{11}F_6P_2ReS_2$	$C_{43}H_{32}O_8Cl_5F_6P_2ReS_2$
fw	819.70	846.83	1156.05	1280.27
cryst dimens, mm	0.25 × 0.15 × 0.35	0.20 × 0.05 × 0.25	0.20 × 0.10 × 0.30	0.20 × 0.10 × 0.30
cryst syst	monoclinic	monoclinic	triclinic	monoclinic
space group	$P2_1/c$ (No. 14)	$P2_1/c$ (No. 14)	$P\bar{1}$ (No. 2)	$P2_1/n$ (No. 14)
a, Å	10.988(2)	15.110(5)	12.447(2)	11.01(1)
b, Å	18.952(2)	14.936(5)	17.396(2)	25.74(1)
c, Å	16.413(3)	16.773(2)	11.595(2)	11.984(10)
α, deg			105.19(1)	
β, deg	102.44(2)	111.34(1)	102.67(1)	93.29(7)
γ, deg			75.80(1)	
V, Å^3	3338.4(9)	3525(1)	2389.5(7)	5090(7)
Z	4	4	2	4
ρ_{calcd}, g cm^{-3}	1.631	1.595	1.607	1.671
abs coeff, cm^{-1}	37.66	35.82	27.77	28.66
$F(000)$	1624	1672	1148	2520
no. of unique data collected	4928	4819	6248	9169
no. of obsd data with $I \geq 3\sigma(I)$	3761	3378	5325	6322
no. of variables	409	442	586	559
R^a	0.034	0.032	0.041	0.042
$R_w{}^b$	0.043	0.035	0.060	0.051
goodness-of-fit, S^c	2.05	1.48	2.43	2.58
$\Delta\rho$(max, min, e Å^{-3})	+0.83, −0.69	+1.20, −0.58	+1.40, −0.75	+1.46, −0.92

^{a} $R = \Sigma(||F_o| - |F_c||)/\Sigma|F_o|$. ^{b} $R_w = [\Sigma w(|F_o| - |F_c|)^2/\Sigma w|F_o|^2]^{1/2}$. ^{c} $S = [\Sigma w(|F_o| - |F_c|)^2/(n - p)]^{1/2}$.

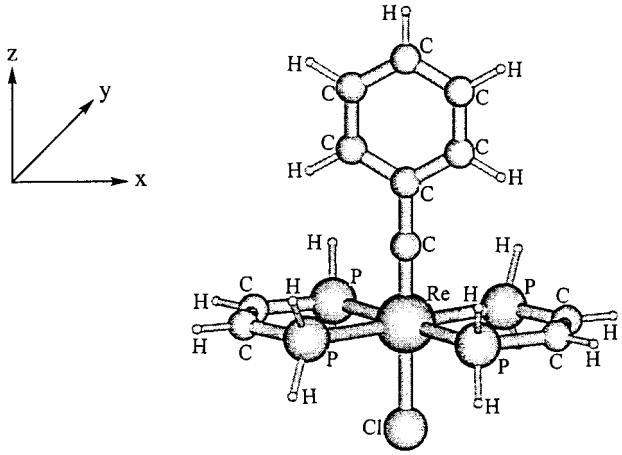

Figure 1. Geometry of the model molecule [Re(≡CC_6H_5)(H_2PCH=$CHPH_2$)$_2$Cl]$^+$ (**2m**).

Molecular-Orbital Calculations. Hartree−Fock self-consistent-field (HF-SCF)[15] and single-excitation configuration interaction (CI-singles)[16] calculations were performed using the Gaussian 94/DEF program package[17] on a Silicon Graphics Indigo 2 workstation.

The symmetry of the model compounds [Re(≡CPh)(H_2PCH=$CHPH_2$)$_2$Cl]$^+$ (**2m**, Figure 1), [Re(≡CPh)(PH_3)$_2$Cl(CO)(OH_2)]$^+$ (**3m**; see Supporting Information), and [Re(≡CPh)(H_2PCH=$CHPH_2$)(CO)$_2$(OH)]$^+$ (**13m**; see Supporting Information) may only be as high as C_{2v}, C_s, and C_s for **2m**, **3m**, and **13m**, respectively, depending on the orientation of ligands. These symmetries were chosen for the calculations because full optimizations for the models indicate that they are the most stable, plus the metrical parameters of the crystal data show that [Re(≡CAr′)(pdpp)$_2$Cl]$^+$ (**2**),[9] [Re(≡CAr′)(PPh_3)$_2$(CO)(H_2O)Cl]$^+$ (**3**),[9] and [Re(≡CC_6H_5Cl-*p*)(pdpp)(CO)$_2$(O_3SCF_3)]$^+$ (**13d**) have virtual C_{2v}, C_s, and C_s symmetry, respectively.

The main optimized bond distances (Å) and angles (deg) are as follows: in **2m** Re≡C 1.76, C−Ph 1.44, Re−Cl 2.54, Re−P 2.52, P−Re−P 81.25; in **3m** Re≡C 1.76, C−Ph 1.43, Re−Cl 2.52, Re−C 1.99, Re−O 2.28; in **13m** Re≡C 1.79, C−Ph 1.43, Re−C 2.04, Re−O 2.01, Re−P 2.57, P−Re−P 80.38, C−Re−C 93.37.

The ab initio calculations utilized the quasirelativistic effective core potential (ECP) developed by Hay and Wadt;[18] only the outermost electrons of each atom were treated explicitly. For the Re atom, this includes electrons in the 5s, 5p, 5d, and 6s orbitals, and for P and Cl, this includes 3s and 3p electrons. All the electrons were included for C, O, and H atoms. The double-ζ valence Gaussian basis set associated with the pseudopotential is adopted. The basis sets were taken as Re (8s6p3d)/[3s3p2d], P (3s3p)/[2s2p], Cl (3s3p)/[2s2p], C (10s5p)/[3s2p], O (10s5p)/[3s2p], and H (4s)/[2s].

Results and Discussion

Synthesis and Characterization. The synthetic strategy[9] used to prepare the 2,4,6-trimethylbenzylidynerhenium(V) complexes [Re(≡CAr′)(pdpp)$_2$Cl]$^+$ (**2**), [Re(≡CAr′)L_2(CO)(H_2O)Cl]$^+$ (L = PPh_3, **3**; P(C_6H_4OMe-*p*)$_3$, **4**; $PMePh_2$, **5**), and [Re(≡CAr′)(dppe)(CO)$_2$Cl]$^+$ (**6**) is also applicable for the synthesis of derivatives containing nitrogen donor ligands: [Re(≡CAr′)(X_2-bpy)(CO)$_2$Cl]$^+$ (X = H, **7**; Cl, **8**; CO_2CH_3, **9**) and [Re(≡CAr′)(Tp′)(CO)$_2$]$^+$ (**10**) are afforded by the treatment of [Re(≡CAr′)(CO)$_4$Cl]$^+$ (**1**) with the corresponding diimine or KTp′. They are the first examples of rhenium benzylidyne complexes supported by nitrogen donors. The IR spectra of **7**−**9** are similar, with two strong CO bands at *ca.* 2090 and 2030 cm^{-1} while the CO bands of **10** appear at 2076 and 2010 cm^{-1}.

Efficient synthesis of the para-substituted benzylidynerhenium(V) compounds [Re(≡CC_6H_4R-*p*)](pdpp)-

(15) Roothan, C. C. J. *Rev. Mod. Phys.* **1951**, *23*, 69. (b) Pople, J. A.; Nesbet, R. K. *J. Chem. Phys.* **1959**, *22*, 571. (c) McWeeny, R.; Dierksen, G. *J. Chem. Phys.* **1968**, *49*, 4852.

(16) Foresman, J. B.; Head-Gorden, M.; Pople, J. A.; Frisch, M. J. *J. Phys. Chem.* **1992**, *96*, 135.

(17) Frisch, M. J.; Trucks, G. W.; Schlegel, H. B.; Gill, P. M. W.; Johnson, B. G.; Robb, M. A.; Cheeseman, J. R.; Keith, T.; Petersson, G. A.; Montgomery, J. A.; Raghavachari, K.; Al-Laham, M. A.; Zakrzewski, V. G.; Ortiz, J. V.; Foresman, J. B.; Cioslowski, J.; Stefanov, B. B.; Nanayakkara, A.; Challacombe, M.; Peng, C. Y.; Ayala, P. Y.; Chen, W.; Wong, M. W.; Andres, J. L.; Replogle, E. S.; Gomperts, R.; Martin, R. L.; Fox, D. J.; Binkley, J. S.; Defrees, D. J.; Baker, J.; Stewart, J. P.; Head-Gordon, M.; Gonzalez, C.; Pople, J. A. *Gaussian 94, Revision C.3*; Gaussian, Inc.: Pittsburgh, PA, 1995.

(18) (a) Hay, P. J.; Wadt, W. R. *J. Chem. Phys.* **1985**, *82*, 270. (b) Schwerdtfeger, P.; Dolg, M.; Schwarz, W. H. E.; Bowmaker, G. A.; Boyd, P. D. W. *J. Chem. Phys.* **1989**, *91*, 1762.

Scheme 1

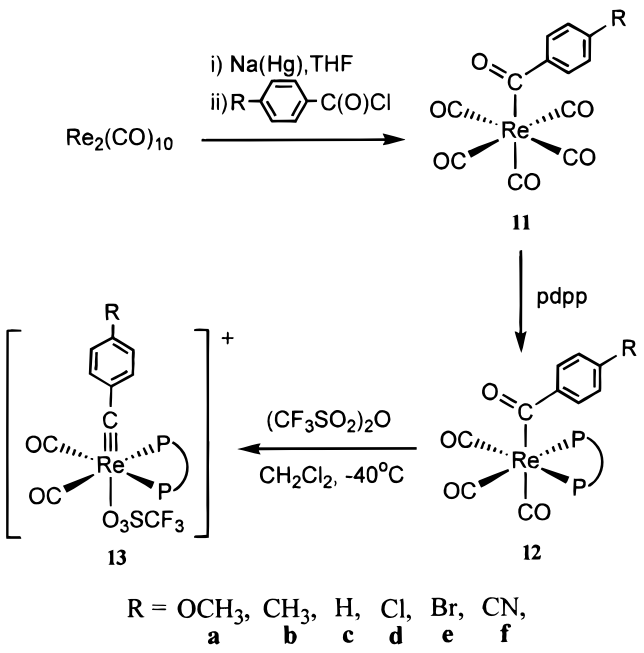

$(CO)_2(O_3SCF_3)][O_3SCF_3]$ (**13**, R = OMe, **a**; Me, **b**; H, **c**; Cl, **d**; Br, **e**; CN, **f**) has been developed by modification of Schrock's method.[8] The para-substituted benzoylrhenium(I) complexes $Re[C(O)C_6H_4R\text{-}p](CO)_5$ (**11a**−**f**) are readily formed from $Re_2(CO)_{10}$, and substitution of CO with pdpp yield the air- and moisture-stable species $Re[C(O)C_6H_4R\text{-}p](pdpp)(CO)_3$ (**12a**−**f**). Trifluoromethanesulfonic anhydride is subsequently used as an oxygen-abstracting reagent to give the series of benzylidyne derivatives **13a**−**f** (Scheme 1).

The IR spectra of benzoylrhenium(I) complexes $Re[C(O)R](CO)_5$ (**11a**−**f**) are comparable and depict a sharp peak at *ca*. 2135 cm^{-1} and a broad band in the 2055−1975 cm^{-1} region for the CO stretching frequencies. In the ^{13}C NMR spectra, no systematic effect by the para-substituents is observed upon the benzoyl resonances, which are located at 242.2−246.0 ppm. The ^{13}C NMR signal for the CO ligand trans to the benzoyl group appears at *ca*. 181 ppm, while those for the four equatorial COs are found at *ca*. 183 ppm. The IR spectra of $Re[C(O)C_6H_4R\text{-}p](pdpp)(CO)_3$ (**12a**−**f**) contains three CO bands at *ca*. 2010, 1940, and 1910 cm^{-1}, which are consistent with a *fac* configuration at the rhenium center. The ^{13}C NMR shifts of the benzoyl carbons (265−268 ppm) and axial (193 ppm) and equatorial (196 and 197 ppm) CO groups are downfield from those of the pentacarbonyl derivatives **11a**−**f**. The IR spectra of $[Re(\equiv CC_6H_4R\text{-}p)](pdpp)(CO)_2(O_3SCF_3)][O_3SCF_3]$ (**13a**−**f**) show CO bands at *ca*. 2110 and 2070 cm^{-1}, while their ^{13}C NMR spectra reveal resonances for the benzylidyne carbon in the 297.6−302.5 ppm range.

Complexes **7**−**9** with substituted bpy ligands are stable for *ca*. 1 month in air in the solid state but decompose after only a matter of days in acetonitrile solution. In contrast, **2**−**6** (containing phosphine ligands) and **10** (with Tp') can be stored in air for several months. Complexes **13a**−**f** are slightly air-sensitive and decompose in aerobic dichloromethane after a few hours at room temperature.

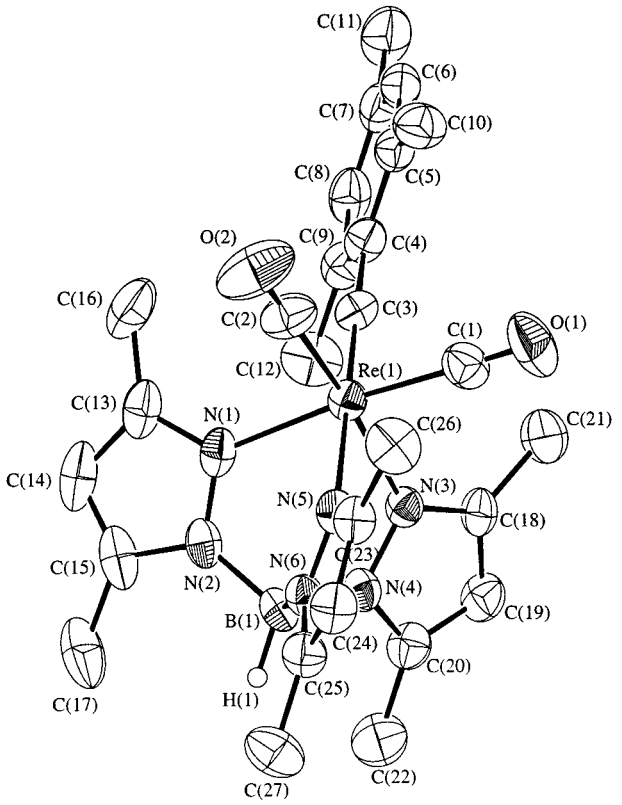

Figure 2. Perspective view of $[Re(CAr')(Tp')(CO)_2]^+$ (**10**; 35% probability ellipsoids).

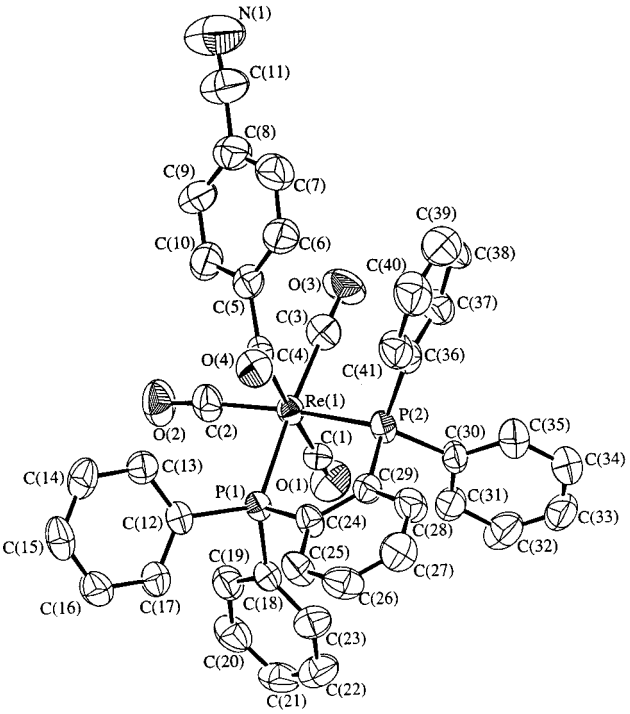

Figure 3. Perspective view of $Re[C(O)C_6H_4CN\text{-}p](pdpp)(CO)_3$ (**12f**; 40% probability ellipsoids).

Crystal Structures. Perspective views of complexes **10**, **12f**, **13a**·CH_3OH·H_2O, and **13d**·$2CH_2Cl_2$ are presented in Figures 2−5, respectively; those of complexes **7**·$CHCl_3$, **12a**, and **12d** are given in the Supporting Information. Selected bond distances and angles are listed in Table 2.

The Re≡C distances in this work (Å; 1.772(7) for **7**,

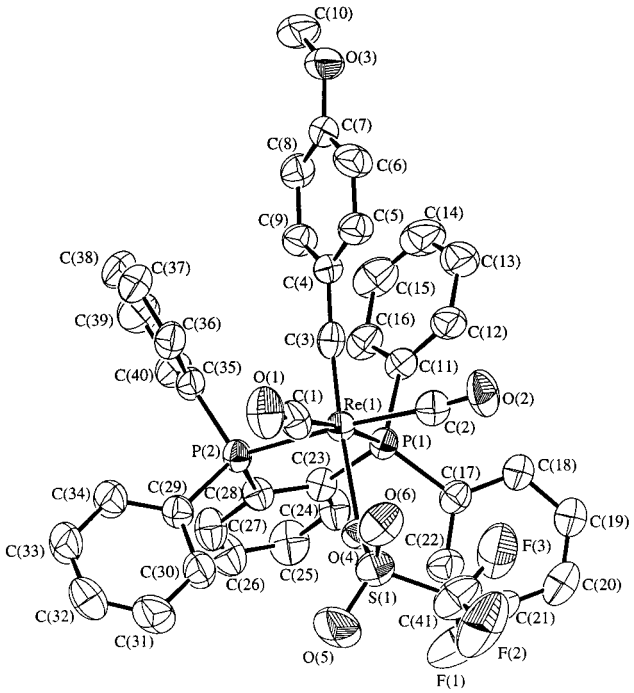

Figure 4. Perspective view of $[Re(\equiv CC_6H_4OMe\text{-}p)(pdpp)(CO)_2(O_3SCF_3)]^+$ (**13a**; 40% probability ellipsoids).

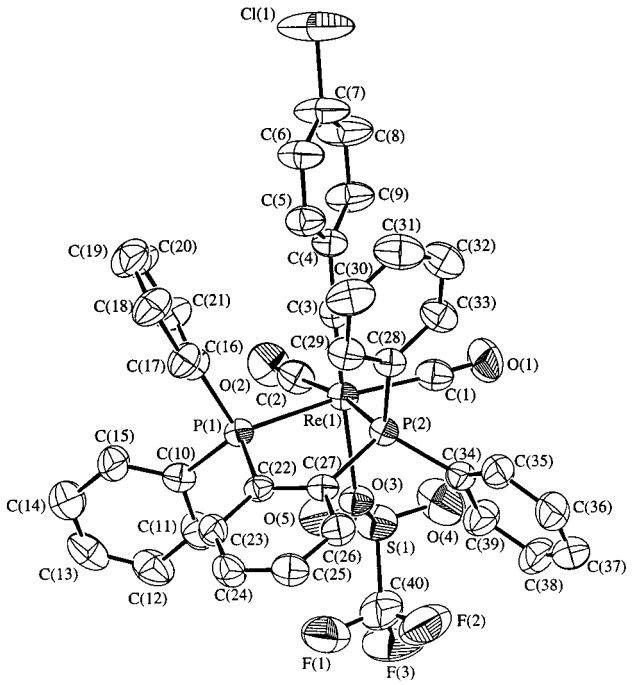

Figure 5. Perspective view of $[Re(\equiv CC_6H_4Cl\text{-}p)(pdpp)(CO)_2(O_3SCF_3)]^+$ (**13d**; 40% probability ellipsoids).

1.786(7) for **10,** 1.769(10) for **13a,** 1.766(8) for **13d**) are typical for rhenium−carbon triple bonds[10] and are comparable to those in the previously reported structures of **2** and **3** (1.802(5) and 1.784(8) Å, respectively).[9] The distances from the benzylidyne carbon to the neighboring *ipso*-carbon (Å; 1.49(2) for **7**, 1.424(10) for **10**, 1.43(1) for **13a**, 1.43(1) for **13d**) are slightly shorter than normal C−C single bonds and suggest π-electron delocalization throughout the Re≡C−Ar moiety (Ar = substituted phenyl). The Re≡C distances also approach those in $[Re(\equiv CCH_2{}^tBu)(dppe)_2F][BF_4]$ (1.772(7) Å),[10j] $[Re(\equiv CNHMe)(dppe)_2Cl][BF_4]$ (1.798(30) Å),[10k] and $[Re(\equiv CNH_2)(dppe)_2Cl][BF_4]$ (1.802(4) Å).[10k] The Re≡C−C_{ipso} angles are all close to linearity as expected.

Table 2. Selected Bond Distances (Å) and Angles (deg) for Complexes 10, 12f, 13a·CH_3OH·H_2O, and 13d·$2CH_2Cl_2$

Compound 10			
Re(1)−N(1)	2.158(6)	Re(1)−C(2)	1.972(9)
Re(1)−N(3)	2.142(5)	Re(1)−C(3)	1.786(7)
Re(1)−N(5)	2.226(6)	C(3)−C(4)	1.424(10)
Re(1)−C(1)	1.962(9)		
N(1)−Re(1)−N(3)	85.6(2)	N(1)−Re(1)−C(3)	96.4(3)
N(1)−Re(1)−N(5)	83.3(2)	N(3)−Re(1)−C(3)	96.9(2)
C(1)−Re(1)−C(3)	90.3(3)	N(5)−Re(1)−C(3)	179.5(3)
C(2)−Re(1)−C(3)	91.4(3)	Re(1)−C(3)−C(4)	178.8(6)
Compound 12f			
Re(1)−P(1)	2.425(2)	C(4)−C(5)	1.54(1)
Re(1)−C(1)	1.952(9)	Re(1)−C(4)	2.199(9)
C(1)−Re(1)−C(4)	176.6(3)	P(1)−Re(1)−C(4)	90.5(2)
C(2)−Re(1)−C(4)	89.5(3)	P(2)−Re(1)−C(4)	83.7(2)
C(3)−Re(1)−C(4)	88.0(3)	Re(1)−C(4)−C(5)	116.7(6)
Compound 13a·CH_3OH·H_2O			
Re(1)−P(1)	2.461(2)	Re(1)−C(3)	1.769(10)
Re(1)−O(4)	2.231(6)	C(3)−C(4)	1.43(1)
P(1)−Re(1)−C(3)	93.5(3)	C(1)−Re(1)−C(3)	89.8(4)
P(2)−Re(1)−C(3)	94.5(3)	C(2)−Re(1)−C(3)	88.5(4)
O(4)−Re(1)−C(3)	175.6(3)	Re(1)−C(3)−C(4)	175.3(7)
Compound 13d·$2CH_2Cl_2$			
Re(1)−P(1)	2.472(2)	Re(1)−C(3)	1.766(8)
Re(1)−O(3)	2.228(5)	C(3)−C(4)	1.43(1)
P(1)−Re(1)−C(3)	94.8(2)	C(1)−Re(1)−C(3)	89.2(3)
P(2)−Re(1)−C(3)	94.6(2)	C(2)−Re(1)−C(3)	89.3(3)
O(3)−Re(1)−C(3)	177.3(3)	Re(1)−C(3)−C(4)	175.9(6)

The substantial trans influence of the benzylidyne ligand is illustrated in these structures. In complex **7**, a trans chloride group (C(3)−Re(1)−Cl(1) 174.7(4)°) results in a rather long Re(1)−Cl(1) distance of 2.485(2) Å, similar to that in **2** (2.497(2) Å).[9] For **10** with the facial Tp′ ligand, the nitrogen atom N(5) trans to the benzylidyne moiety (N(5)−Re(1)−C(3) 179.5(3)°) is located further from the metal center (Å; Re(1)−N(5) 2.226(6), *cf.* Re(1)−N(1) 2.158(6), Re(1)−N(3) 2.142(5)). For **13a** and **13d**, a relatively long Re−O contact to the trans triflate group is revealed in each case (Å; 2.231(6) for **13a**, 2.228(5) for **13d**).

The structures of the benzoyl complexes **12a**, **d**, and **f** are similar, and depict a distorted octahedral configuration. The benzoyl ligand is trans to one of the three CO groups with virtually linear C(1)−Re(1)−C(4) angles (176.5(2)° for **12a**, 177.2(2)° for **12d**, and 176.6(3)° for **12f**). The angles around the benzoyl carbon C(4) approach 120°, as expected for sp^2 hybridization (for example, in complex **12f** Re(1)−C(4)−C(5) 116.7(6)°, Re(1)−C(4)−O(4) 128.2(7)°, C(5)−C(4)−O(4) 115.0(8)°).

Absorption Spectra and Electronic Structures. The UV−vis absorption data of the benzylidyne complexes are summarized in Table 3. The absorption spectra of $[Re(\equiv CAr')(pdpp)_2Cl]^+$ (**2**), $[Re(\equiv CAr')(PR_3)_2(CO)(H_2O)Cl]^+$ **(3−5),** $[Re(\equiv CAr')(dppe)(CO)_2Cl]^+$ (**6**), $[Re(\equiv CAr')(Tp')(CO)_2]^+$ (**10**), and $[Re(\equiv CC_6H_4\text{−}R)(pdpp)(CO)_2(O_3SCF_3)]^+$ (**13a**−**f**) possess similar features: an intense band in the 310−354 nm region and weak absorption in the 370−430 nm range. The absorption spectrum of **13c** is shown in Figure 6. We note that complex **13a** displays an intense peak at 351 nm, but inexplicably, no other lower energy absorptions are

Table 3. UV−Vis Spectral Data of Benzylidyne Complexes at Room Temperature[a]

complex	λ_{max},[c] nm (ϵ_{max},[d] dm^3 mol^{-1} cm^{-1})
2 [Re(≡CAr′)(pdpp)$_2$Cl]$^+$	318 (13 900), 410 (450)
3 [Re(≡CAr′)(PPh$_3$)$_2$(CO)(H$_2$O)Cl]$^+$	321 (13 900), 410 (1380)
4 [Re(≡CAr′){P(C$_6$H$_4$OMe-*p*)$_3$}$_2$(CO)(H$_2$O)Cl]$^+$	320 (13 100), 420 (320)
5 [Re(≡CAr′)(PPh$_2$Me)$_2$(CO)(H$_2$O)Cl]$^+$	320 (12 100), 410 (470)
6 [Re(≡CAr′)(dppe)(CO)$_2$Cl]$^+$	330 (7290), 430 (400)
7 [Re(≡CAr′)(bpy)(CO)$_2$Cl]$^+$ [b]	231 (31 500), 260 (20 300) 313 (22 400), 320 (24 000) 340 (16 400)
8 [Re(≡CAr′)(Cl$_2$-bpy)(CO)$_2$Cl]$^+$	262 (22 200), 310 (17 700) 318 (20 800), 346 (15 800)
9 [Re(≡CAr′){(CO$_2$Me)$_2$-bpy}(CO)$_2$Cl]$^+$	253 (20 800), 330 (23 600) 337 (26 200), 390 (9560)
10 [Re(≡CAr′)(Tp′)(CO)$_2$]$^+$	354 (15 400), 425 (970)
13a [Re (≡CC$_6$H$_4$OMe)(pdpp)(CO)$_2$(O$_3$SCF$_3$)]$^+$	351 (25 200)
13b [Re(≡CC$_6$H$_4$Me)(pdpp)(CO)$_2$(O$_3$SCF$_3$)]$^+$	326 (18 700), 425(300)
13c [Re(≡CC$_6$H$_5$)(pdpp)(CO)$_2$(O$_3$SCF$_3$)]$^+$	310 (14 800), 425 (580)
13d [Re(≡CC$_6$H$_4$Cl)(pdpp)(CO)$_2$(O$_3$SCF$_3$)]$^+$	325 (19 200), 370 (1440)
13e [Re(≡CC$_6$H$_4$Br)(pdpp)(CO)$_2$(O$_3$SCF$_3$)]$^+$	329 (23 200), 375 (3170)
13f [Re(≡CC$_6$H$_4$CN)(pdpp)(CO)$_2$(O$_3$SCF$_3$)]$^+$	313 (18 900), 380 (860)

[a] In CH_2Cl_2 unless otherwise stated. [b] In MeCN. [c] Error ±2 nm. [d] Error ±1 in last significant figure.

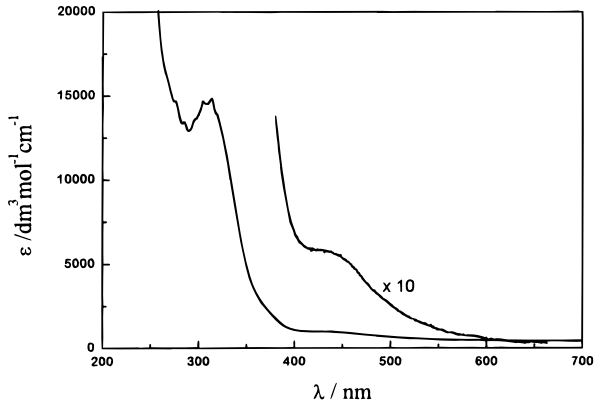

Figure 6. UV−vis absorption spectrum of [Re(≡CC$_6$H$_5$)(pdpp)(CO)$_2$(O$_3$SCF$_3$)]$^+$ (**13c**) in CH_2Cl_2 at room temperature.

observed even at a concentration of 5×10^{-3} mol dm^{-3}. Although it is difficult to precisely define the energy of the lowest energy absorption shoulder, it is apparent from Table 3 that the different electron-withdrawing para-substituents in complexes **13d**−**f** cause a gradual blue shift (ca. 3500 cm^{-1}).

Complex **10** containing Tp′ displays a significant red shift to 354 nm for the high-energy band. Significantly, the absorption spectra of **7**−**9** containing para-substituted bipyridine are different from the other benzylidyne complexes in this work. A strong peak ($\epsilon > 2 \times 10^4$ dm^3 mol^{-1} cm^{-1}) centered at 320, 318, and 337 nm for **7**, **8**, and **9**, respectively, is observed and is accompanied by a higher energy shoulder. The lowest energy absorption appears at *ca*. 340, 346, and 390 nm for **7**, **8**, and **9**, respectively, and is also intense ($\epsilon > 1.5 \times 10^4$ dm^3 mol^{-1} cm^{-1}).

In solvent-dependent UV−vis studies on complexes **2** and **10**, no significant shifts were observed when the solvent is changed from chloroform to acetonitrile. The absorption spectra of **13e** in different solvents showed significant but irregular changes, and this is ascribed to the activity of the coordinated triflate group. A solvent effect on the electronic absorption bands of this class of Re(V) benzylidyne complexes is, therefore, discounted.

As an aid to interpreting the electronic absorption spectra, HF-SCF calculations[15] have been performed on the model molecules [Re(≡CC$_6$H$_5$)(H$_2$PCH═CHPH$_2$)$_2$Cl]$^+$ (**2m**, Figure 1; *x*, *y*, *z* axis defined), [Re(≡CC$_6$H$_5$)(PH$_3$)$_2$(CO)(H$_2$O)Cl]$^+$ (**3m**; see Supporting Information), and [Re(≡CC$_6$H$_5$)(H$_2$PCH═CHPH$_2$)(CO)$_2$(OH)]$^+$ (**13m**; see Supporting Information). The calculated energy and composition of the near frontier orbitals for **2m**, **3m**, and **13m** are summarized in the Supporting Information and reveal that the HOMO for each complex (for **2m**, Figure 7 bottom) is the π(Re≡C−Ph) orbital with π bonding between d_{xz}(Re) and p_x(≡C) (**2m** d_{xz} 27.96%, p_x(≡C) 6.93%, p_x(Ph) 34.94%; **3m** d_{xz} 32.65%, p_x(≡C) 1.89%, p_x(Ph) 59.33%; **13m** d_{xz} 26.83%, p_x(≡C) 4.03%, p_x(Ph) 35.63%). This is different from previous assignments of the HOMO in related tungsten complexes to a metal d orbital that is nonbonding with respect to the benzylidyne ligand.[4,5] The LUMO (for **2m**, Figure 7 (top)) is a π^*(Re≡C−Ph) orbital with antibonding between d_{xz}(Re) and p_x(≡C) (**2m** d_{xz} 20.49%, p_x(≡C) 21.19%, p_x(Ph)

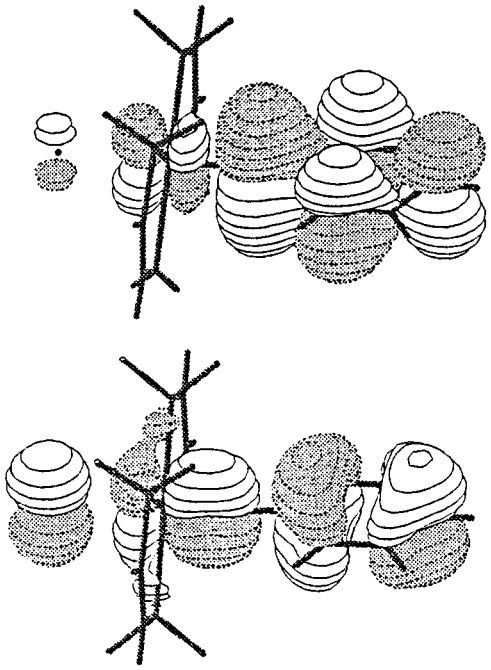

Figure 7. HOMO (bottom) and LUMO (top) of **2m**. Coefficients are derived from the HF calculation.

Table 4. Luminescence Data for Benzylidyne Complexes at Room Temperature[a]

complex	λ_{max}, nm[c]	ϕ_{em}[d]	τ, μs[d]
2 [Re(≡CAr′)(pdpp)$_2$Cl]$^+$	573	0.042	2.08
3 [Re(≡CAr′)(PPh$_3$)$_2$(CO)(H$_2$O)Cl]$^+$	580	0.0020	2.25
4 [Re(≡CAr′){P(C$_6$H$_4$OMe-*p*)$_3$}$_2$(CO)(H$_2$O)Cl]$^+$	588	0.0067	1.76
5 [Re(≡CAr′)(PPh$_2$Me)$_2$(CO)(H$_2$O)Cl]$^+$	611	0.0046	0.95
6 [Re(≡CAr′)(dppe)(CO)$_2$Cl]$^+$	567	0.0035	3.35
7 [Re(≡CAr′)(bpy)(CO)$_2$Cl]$^+$ [b]	555	0.00025	0.43
8 [Re(≡CAr′)(Cl$_2$-bpy)(CO)$_2$Cl]$^+$	575	0.00012	0.07
9 [Re(≡CAr′){(CO$_2$Me)$_2$-bpy}(CO)$_2$Cl]$^+$	580	0.0028	0.61
10 [Re(≡CAr′)(Tp′)(CO)$_2$]$^+$	585	0.0027	1.48
13a [Re(≡CC$_6$H$_4$OMe)(pdpp)(CO)$_2$(O$_3$SCF$_3$)]$^+$	520	0.00015	0.02
13b [Re(≡CC$_6$H$_4$Me)(pdpp)(CO)$_2$(O$_3$SCF$_3$)]$^+$	527	0.0018	0.22
13c [Re(≡CC$_6$H$_5$)(pdpp)(CO)$_2$(O$_3$SCF$_3$)]$^+$	530	0.0026	0.53
13d [Re(≡CC$_6$H$_4$Cl)(pdpp)(CO)$_2$(O$_3$SCF$_3$)]$^+$	536	0.012	2.18
13e [Re(≡CC$_6$H$_4$Br)(pdpp)(CO)$_2$(O$_3$SCF$_3$)]$^+$	537	0.011	2.42
13f [Re(≡CC$_6$H$_4$CN)(pdpp)(CO)$_2$(O$_3$SCF$_3$)]$^+$	559	0.016	4.84

[a] λ_{ex} = 300−350 nm; in CH_2Cl_2 unless otherwise stated. [b] In MeCN. [c] Error ±2 nm. [d] Error ±10%.

49.02%; **3m** d_{xz} 21.56%, p_x(≡C) 26.39%, p_x(Ph) 42.04%; **13m** d_{xz} 18.61%, p_x(≡C) 26.30%, p_x(Ph) 43.31%). By comparing the composition of these orbitals, we find that the percentage of d_{xz} in the LUMO is smaller than that in the HOMO whereas the percentage of p_x(≡C) increases tremendously in the LUMO. Hence, if the lowest energy transition involves these frontier orbitals, then this can be formulated as π(Re≡C−Ph) → π*(Re≡C−Ph) with $d_{xz} \rightarrow p_x$(≡C) MLCT character, where the p_x(≡C) orbital and phenyl π system are conjugated.

To aid in the assignment of the transitions in the absorption spectra of these complexes, a CI-singles calculation[16] was performed on the excited states of the optimized model molecule **2m** (see Supporting Information), where all the orbitals and electrons of the ground state were included to take into account the electronic correlation for the excited states. The calculated lowest energy absorption at 461 nm (HOMO to LUMO triplet transition, see Supporting Information) can be visualized as a spin-forbidden transition of π(Re≡C−Ph) → π*(Re≡C−Ph) (*vide supra*). From the absorption spectrum of **2**, a weak shoulder at *ca*. 410 nm is assigned to this transition. In addition, the calculated HOMO to LUMO singlet transition at 290 nm correlates with the 318 nm band in the absorption spectrum.

On the basis of these calculations, the lowest energy absorption for the rhenium(V) benzylidyne complexes **2**−**6**, **10**, and **13a**−**f** can be assigned to a ^{3}[π(Re≡CAr) → π*(Re≡CAr)] transition and the higher energy band to ^{1}[π(Re≡CAr) → π*(Re≡CAr)]; both of these contain notable d(Re) → p(≡C) MLCT character, and the p_x(≡C) orbital and phenyl π system are conjugated. Furthermore, if this is correct, the energies of these two absorption bands should be affected by substituents on the benzylidyne ligand but relatively insensitive to different auxiliary ligands. This is indeed consistent with our observation that while the variation of phosphine ligands only alters the absorption bands of complexes **2**−**6** to a small extent, the nature of the para-substituents on the benzylidyne ligand in **13a**−**f** significantly affects the absorption energies (Table 3). The fact that the absorption bands are not solvent-dependent is consistent with the proposal that the electronic transitions are not pure MLCT.

The UV−vis absorption spectra of complexes **7**−**9** containing 4,4′-substituted bipyridine ligands are different, and hence the above assignment of the electronic transitions is not applicable. The spectral features of these complexes resemble those for a series of rhenium(I) N-heterocyclic carbene complexes containing 4,4′-substituted bipyridine ligands, [HNCH$_2$CH$_2$NHCRe(X$_2$-bpy)(CO)$_3$]$^+$, where the absorption peaks at 350−400 nm are assigned to a [d(Re) → π*(X$_2$-bpy)] ^{1}MCLT transition, and a correlation between the ^{1}MLCT transition energy and the Hammett parameters (σ) of the substituents X was demonstrated.[19] We therefore tentatively assign the lowest energy shoulders of complexes **7**−**9** to the [d(Re) → π*(X$_2$-bpy)] ^{1}MLCT transition. Electron-withdrawing substituents such as CO_2CH_3 should lower the π*(X$_2$-bpy), and thus the absorption energy, and correspondingly, the lowest energy absorption of complex **9** containing (CH$_3$O$_2$C)$_2$-bpy appears at *ca*. 390 nm compared with that for **7** (340 nm) and **8** (346 nm).

Luminescence Studies and Modification of Excited-State Properties. All of the rhenium(V) benzylidyne complexes emit in fluid solution at room temperature upon excitation at 300−350 nm (Table 4). The profile of their emission spectra are very similar: a broad and structureless band which is indicative of a large degree of vibrational coupling like the solution emission of [Ru(bpy)$_3$]$^{2+}$.[20] The emission energies λ_{max} range from 520 to 610 nm, and the emission lifetimes vary from 0.02 to 4.84 μs. The relatively long lifetimes imply that the transitions involved are spin-forbidden. The emitting states of these complexes are assigned to the lowest energy transition. For **2**−**6**, **10**, and **13a**−**f**, the lowest energy excited states have been identified as ^{3}[π(Re≡CAr) → π*(Re≡CAr)] (*vide supra*). This assignment predicts that the excited-state energy is affected by the electronic properties of the benzylidyne group, and changing the para-substituents would affect both the π(Re≡CAr) and π*(Re≡CAr) energies. Electron-donating substituents such as OCH_3 and CH_3 should lower the energy of π(Re≡CAr) and raise that of π*(Re≡CAr) and consequently increase the energy gap. Conversely, electron-withdrawing substituents such as Cl, Br, and CN should reduce this gap. Thus, a correlation between the emission energy of **13a**−**f** and the Hammett parameters (σ) of the benzylidyne para-substituents is anticipated and indeed observed (Figure 8). This demonstrates that the emission energy of these derivatives can be tuned and implies (1) association

(19) Xue, W. M.; Chan, M. C. W.; Su, Z. M.; Cheung, K. K.; Liu, S. T.; Che, C. M. *Organometallics* **1998**, *17*, 1622.
(20) Lytle, F. E.; Hercules, D. M. *J. Am. Chem. Soc.* **1969**, *91*, 253.

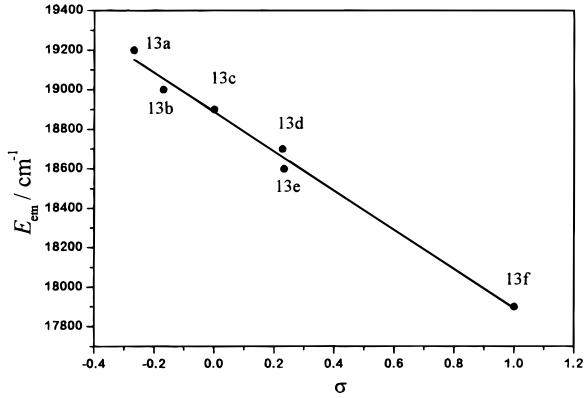

Figure 8. Correlation plot of room-temperature emission energy E_{em} vs Hammett parameters σ of the substituents for complexes [Re(≡CC_6H_4R-*p*)(pdpp)$(CO)_2(O_3SCF_3)$]$^+$ (**13a**−**f**), $R = -0.99$, slope = -993 ± 49.

between the emitting state and the benzylidyne moiety and (2) delocalization of π(Re≡C) and π^*(Re≡C) into the phenyl π system. The tunable range of the excited-state energy is 1300 cm^{-1}. This is the first example of systematic modification of the excited-state energy of metal benzylidyne complexes by variation of the benzylidyne moiety.

In addition to effects on emission energy, the variation of benzylidyne and the auxiliary ligands also influences the emission lifetime and quantum yield. As shown in Table 4, lifetimes in the 20 ns to 4.8 μs range and quantum yields from 1.2×10^{-4} up to 4.2×10^{-2} are observed, and these indicate that the nature of the ligands has considerable influence on the excited-state decay kinetics. For complexes **2**−**6** with the (≡CAr′) moiety, the nonradiative decay rate constants increase as excited-state energies decrease, and this is consistent with the energy-gap law as described previously.[9,21]

We have assigned the lowest energy transition and, hence, the emitting state of complexes **7**−**9** containing 4,4′-substituted bipyridine ligands to d(Re) → $\pi^*(X_2\text{-bpy})$ MLCT. The red shift of the emission bands from **7** (555 nm) to **8** (575 nm) and **9** (580 nm), which bear more electron-withdrawing substituents, is consistent with this. Mayr reported that replacing tmen by bipyridine in the tungsten derivative [W(≡CPh)(tmen)$(CO)_2$Cl] totally quenched the fluid solution emission.[1]

At 77 K, the Re(V) complexes [Re(≡$CCH_2C_6H_4$R-*p*)$(dppe)_2$Cl][BF_4] (R = H, Me)[10j] with unconjugated alkylidyne groups were found to emit at 545 and 535 nm, respectively.[22] These are comparable to the emission energies of the benzylidyne complexes (Table 4) and hence this implies that the emitting state is associated with the [Re≡C] moiety. The effect of different solvents on the emissive behavior of complexes **2**, **10**, and **13e** were studied, but like the absorptions, no notable effects were seen upon the emission energies, quantum yields, and lifetimes for **2** and **10**. An irregular effect on the luminescence of **13e** was observed, but again the activity of the coordinated triflate is the likely cause.

The 77 K emission spectra of the benzylidyne complexes show well to poorly resolved vibrational structures. The corrected emission spectra of **13f** in the solid state at 77 K and in dichloromethane solution at room temperature are shown in Figure 9. To our knowledge, this is the first observation of vibronic emission in metal alkylidyne complexes. Gaussian deconvolution of the vibronic structured 77 K emission spectra can be used to obtain the vibrational spacing $\hbar\omega_M$, excited-state distortion S_M, $\nu'_M = 0 \rightarrow \nu_M = 0$ emission energy E_{em}(0−0), and full-width at half-maximum of the individual vibrational components $\tilde{\nu}_{1/2}$.[23] The fitting results are available in the Supporting Information and show vibrational progression $\hbar\omega_M$ between 1080 and 1218 cm^{-1} and excited-state distortion S_M in the 1.21−1.72 range. The latter indicate that the emitting states are not pure MLCT, for which S_M values are typically *ca.* 1.0.[24]

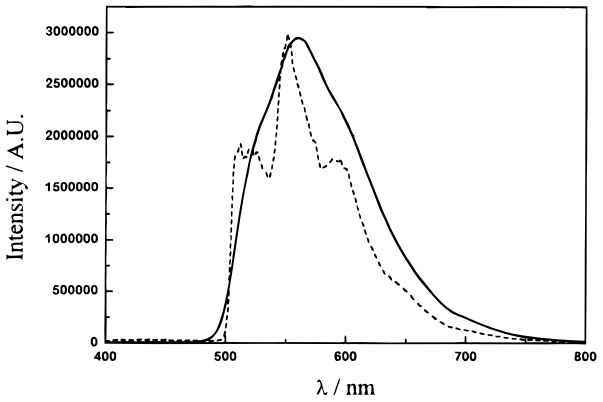

Figure 9. Corrected emission spectra of [Re(≡CC_6H_4CN)(pdpp)$(CO)_2(O_3SCF_3)$]$^+$ (**13f**) in CH_2Cl_2 at room temperature (—) and in solid state at 77K (- - -), λ_{ex} 310 nm, emission intensities are normalized.

Table 5. Electrochemical Data[a]

complex	E_{ox}, V	E_{red}, V
2[b,c]	1.48 [d,h]	
3[b]	1.83,[e] 1.39 [d,h]	−1.31 [f]
4[b]	1.50,[e] 1.31[d]	−1.76 [f]
5[b]	1.78,[e] 1.51[d]	−1.72 [f]
6		−1.20,[g] −1.54 [f]
13a		−0.89,[g] −1.91 [f]
13b		−0.81,[g] −1.84 [f]
13c		−0.77,[g] −1.81 [f]
13d		−0.75,[g] −1.80 [f]
13e		−0.68,[g] −1.67,[f] −1.81
13f		−0.53,[g] −1.51 [f,h]

[a] Measured in CH_2Cl_2 vs SCE; error ±0.02 V; irreversible (E_{pa} and E_{pc} potentials for anodic oxidation and cathodic reduction waves, respectively) unless otherwise stated. [b] In MeCN. [c] Reference 9. [d] Re(VI)/(V). [e] Phosphine oxidation. [f] Benzylidyne reduction. [g] Re(V)/(IV). [h] Reversible.

Electrochemistry. Cyclic voltammetry was used to study the electrochemistry of the benzylidyne complexes (Table 5). The cyclic voltammograms of **3**−**5** are similar and reveal two oxidations and one reduction, all of which are irreversible. The first oxidation is tentatively assigned to Re(V)/Re(VI), and the second is assigned to oxidation of the phosphine ligands. The reduction is ascribed to occur at the benzylidyne ligand.

(21) (a) Englman, R.; Jortner, J. *Mol. Phys.* **1970**, *18*, 145. (b) Freed, K. F.; Jortner, J. *J. Chem. Phys.* **1970**, *52*, 6272.
(22) Xue, W. M.; Che, C. M.; Pombeiro, A. J. L. Unpublished results.
(23) Caspar, J. V.; Meyer, T. J. *J. Am. Chem. Soc.* **1983**, *105*, 5583.
(24) (a) Dressick, W. J.; Cline, J., III; Demas, J. N.; DeGraff, B. A. *J. Am. Chem. Soc.* **1986**, *108*, 7567. (b) Caspar, J. V.; Westmoreland, T. D.; Allen, G. H.; Bradley, P. G.; Meyer, T. J.; Woodruff, W. H. *J. Am. Chem. Soc.* **1984**, *106*, 3492. (c) Allen, G. H.; White, R. P.; Rillema, D. P.; Meyer, T. J. *J. Am. Chem. Soc.* **1984**, *106*, 2613. (d) Casper, J. V.; Meyer, T. J. *Inorg. Chem.* **1983**, *22*, 2444. (e) Lumpkin, R. S.; Meyer, T. J. *J. Phys. Chem.* **1986**, *90*, 5307. (f) Kober, E. M.; Casper, J. V.; Lumpkin, R. S. *J. Phys. Chem.* **1986**, *90*, 3722.

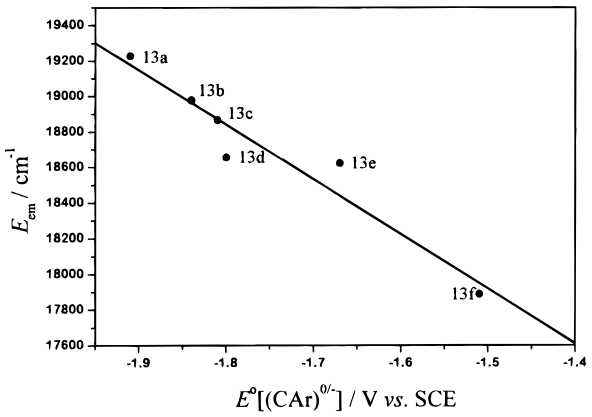

Figure 10. Plot of room-temperature emission energy E_{em} vs ground-state reductive potential $E°[(CAr)^{0/-}]$ for [Re(≡C-C_6H_4R-*p*)(pdpp)$(CO)_2(O_3SCF_3)]^+$ (**13a**−**f**), $R = -0.96$, slope $= -3068 \pm 422$.

No oxidation wave is observed for complexes **6** and **13a**−**f**, which contain two coordinated CO groups, even up to 2.3 V vs SCE. Two irreversible reduction waves (the second for **13f** is reversible) are observed; they are tentatively assigned to metal-centered (Re(V) → Re(IV)) and benzylidyne ligand reductions, respectively.

The electrochemical data of **13a**−**f** provide further support for the assignment of the π^*(Re≡CAr) excited state. Reduction of the benzylidyne group results in addition of an electron into the π^*(≡CAr) orbital. If the emitting state is associated with π^*(≡CAr), a linear relationship should exist between the emission energy (E_{em}) and the reductive potential for the benzylidyne group ($E°[(CAr)^{0/-}]$, denoted with footnote *f* in Table 5). This is indeed observed for complexes **13a**−**f** (Figure 10). Importantly, this correlation illustrates that the excited state is associated with the benzylidyne group and that emission in this system is occurring from states which have a common electronic origin.

Conclusion

Synthetic routes to rhenium(V) benzylidyne complexes have been developed so that both benzylidyne and auxiliary ligands can be conveniently modified, and this has paved the way for exploring the excited-state properties of these luminescent compounds. Data from electronic absorption and emission spectra, electrochemistry, and molecular-orbital calculations provide compelling evidence to suggest that the excited state is [π(Re≡CAr) → π^*(Re≡CAr)] with d(Re) → p(≡C) MLCT character, where the p(≡C) orbital and phenyl π system are conjugated. Significantly, the excited-state properties associated with this chromophore can be tuned by varying the benzylidyne and auxiliary ligands. Hence, the emission energy can be modified from 520 to 610 nm in CH_2Cl_2, a range of 2840 cm^{-1}. The excited-state lifetimes can be adjusted from 20 ns to 4.84 μs, many of which are significantly longer than those in related Mo, W,[1,2] and Os[3] alkylidyne systems, so that Stern−Volmer kinetic experiments are possible.

Acknowledgment. We are indebted to Prof. A. J. L. Pombeiro for providing samples of [Re(≡C$CH_2C_6H_4$R-*p*)$(dppe)_2$Cl][BF_4] (R = H, Me) and for helpful discussions. We thank The University of Hong Kong, the Croucher Foundation, and the Hong Kong Research Grants Council for financial support. M.C.-W.C. is grateful for a University Postdoctoral Fellowship from The University of Hong Kong.

Supporting Information Available: Tables of crystal data, atomic coordinates, calculated hydrogen coordinates, anisotropic displacement parameters, and bond distances and angles for **7**·$CHCl_3$, **10**, **12a**, **12d**, **12f**, **13a**·CH_3OH·H_2O, and **13d**·$2CH_2Cl_2$, the HF-SCF calculated energy and composition of the near frontier orbitals for **2m**, **3m**, and **13m**, excited state assignment of **2m** by CI-singles calculation, analytical data for all complexes, emission parameters calculated from Gaussian deconvolution, and geometry of **2m**, **3m**, and **13m** (99 pages). Ordering information is given on any current masthead page.

OM971054T